CERN-TH/96-124
Bielefeld-TP 96/20
JYFL 96-8

Minijet and Transverse Energy Production in the BFKL Regime

K.J. Eskola[1]
CERN, Theory Division, CH-1211 Geneva 23, Switzerland
email: kjeskola@mail.cern.ch

A.V. Leonidov[2]
Theoretische Physik, Fakultät für Physik,
Universität Bielefeld, D-33615 Bielefeld, Germany
email: andrei@physik.uni-bielefeld.de

P.V. Ruuskanen
Department of Physics, University of Jyväskylä,
P.O. Box 35, FIN-40352 Jyväskylä, Finland
email: ruuskanen@jyfl.jyu.fi

Abstract

Minijet production in hadronic and nuclear collisions through a BFKL pomeron ladder is studied for the energies of the future LHC heavy-ion collisions. We use unintegrated gluon densities compatible with the small-x increase of parton distributions observed at HERA. We show that at LHC energies the BFKL minijet and transverse energy production is at most of the same order of magnitude as that in the collinear factorization approach.

CERN-TH/96-124
June 1996

[1]On leave of absence from Laboratory of High Energy Physics, Department of Physics, University of Helsinki, Finland

[2]Alexander von Humboldt Fellow, on leave from Lebedev Physics Institute, 117924 Leninski pr. 53, Moscow, Russia

Semihard parton scatterings with transverse momenta $p_{\rm T} \sim$ few GeV have been suggested to explain the rapid growth of the inelastic and total cross sections in high energy $pp(\bar{p})$ collisions at $\sqrt{s} > 20$ GeV [1, 2]. Especially in heavy-ion collisions at very high energies the semihard processes are expected to be abundant and dominate the transverse energy production in the central rapidity region [3]. Event generators emphasizing the importance of semihard processes in ultrarelativistic heavy-ion collisions at $\sqrt{s} \geq 200$ AGeV have also been actively developed during recent years [4, 5].

Perturbative processes take place at the very early stages of the time evolution of an ultrarelativistic heavy-ion collision [6]. In the central rapidity region, these semihard processes occur at time scales $\tau \sim 1/p_{\rm T}$, *i.e.* within the first fractions of fm/c, while the particle production from soft processes is expected to take longer, ~ 1 fm/c. Therefore, semihard particle production and associated transverse energy production give initial conditions for further space-time evolution of the formed partonic system, which eventually may lead to a thermalized quark-gluon plasma if the produced system is dense enough. The key feature of the semihard parton production is that it can be computed by using perturbative QCD [3, 6].

At central rapidities the semihard scatterings with momentum exchanges $p_{\rm T} \sim 2$ GeV probe typically parton distributions at $x \sim 2p_{\rm T}/\sqrt{s}$. Especially in nuclear collisions at the CERN Large Hadron Collider (LHC) with $\sqrt{s} =$ 5.5 TeV, these x-values fall dominantly in the region of a rapid increase of the structure function $F_2^p(x, Q^2)$ as observed in deep inelastic ep collisions at HERA [7]. This increase persists down to $Q^2 = 1.5$ GeV^2 [8], thus strongly enhancing production of semihard partons as discussed in [9]. Nuclear effects in the parton distributions, in particular the observed nuclear shadowing of $F_2^A(x, Q^2)$ at small x [10], are expected to be important, although the nuclear gluon distributions are not well known at the moment [11, 12].

In the above-mentioned studies, the production mechanism of semihard partons, minijets, is based on multiple independent $2 \to 2$ scatterings of partons. Collinear factorization is assumed to hold, enabling separation of the perturbatively calculable hard processes from the parton distributions containing non-perturbative input. In the leading twist approximation, the actual hard scattering involves only on-shell partons. In this paper, we will study a different mechanism for minijet production, which is not based on collinear factorization.

The small-x increase of F_2^p measured at HERA can be explained by the Leading Log $(\log Q^2)$ DGLAP-approach [13], by the Double Leading Log $(\log Q^2 \log 1/x)$ approximation [14], or by the Leading Log $(\log 1/x)$ BFKL-approach [15, 16, 17]. In this study, we adopt the BFKL standpoint. Based on this we aim to study minijet and transverse energy production from a colour

singlet (cut) BFKL ladder spanned between the two colliding nuclei. We will not make any attempt to include nuclear effects here and, accordingly, our conclusions for the minijet cross sections should hold for pp collisions as well. The basic difference from the previous minijet studies including collinearly factorized $2 \to 2$ on-shell parton scatterings only [9], is that we now consider production of semihard gluons emitted by the virtual gluons in the legs of the BFKL ladder ordered strongly in rapidity, *i.e.* essentially from $2 \to 1$ parton processes. This mechanism of minijet production was first suggested in [18, 19]. As a new feature, we use the unintegrated gluon distributions directly normalized to the integrated gluon distributions, which exhibit a small-x rise compatible with HERA results [20]. Finally, we compare our results with the more conventional calculation [9] based on collinear factorization. Our conclusion is that the minijet and transverse energy production via the BFKL mechanism is at most of the same order of magnitude as the conventional one.

Minijet production in hadronic collisions from a BFKL ladder in the case of two tagging (mini)jets separated by a wide rapidity gap was studied in [21, 22] and more recently in [23, 24]. A closely related subject in deep inelastic scattering (DIS) is the transverse energy flow due to minijets from the BFKL ladder [25, 26]. Conceptually related to our study in this paper may also be the studies in [27], where collisions of two virtual gluon clouds are considered in the high energy heavy-ion collisions. Finally, let us also mention Ref. [28], where minijet production by a usual soft pomeron is discussed.

As a starting point for our problem, it is useful to recall inclusive minijet production in hadron collisions from a (cut) BFKL ladder as considered in [21] in the case of two tagging jets with a large rapidity gap in between. The situation on the parton level is illustrated in Fig. 1, where the transverse momenta of the tagging jets are denoted by $\mathbf{k}_{a\mathrm{T}}$, $\mathbf{k}_{b\mathrm{T}}$, and rapidities at the hadron CMS by y_a, y_b with $y_a \gg y_b$. The building blocks of such a ladder are the reggeized gluon propagators illustrated by the thick lines and the non-local gauge-invariant effective Lipatov vertices represented by the black blobs in the legs of the ladder. Squaring and summing all the $gg \to (n+2)g$ amplitudes in the leading $\log(\hat{s}/\hat{t})$ approximation leads then in the multi-Regge kinematics to a hard pomeron, *i.e.* to a strongly rapidity-ordered perturbative colour singlet gluon ladder, denoted by $f(\mathbf{q}_{\mathrm{T}}, \mathbf{k}_{\mathrm{T}}, y_a - y_b)$ in Fig. 1. Note that in the multi-Regge kinematics, only the transverse momenta of the legs of the ladder become important, so that $q^2 \approx -\mathbf{q}_{\mathrm{T}}^2 \equiv -q_{\mathrm{T}}^2$. Also, when intrinsic transverse momenta of the incoming partons are neglected, we have $\mathbf{q}_{\mathrm{T}} = -\mathbf{k}_{a\mathrm{T}}$ and $\mathbf{k}_{\mathrm{T}} = \mathbf{k}_{b\mathrm{T}}$. An addition of a rung to the pomeron ladder is governed by an inhomogeneous BFKL equation [15, 16]. For details, we refer to the lecture notes of Del Duca [29], here we merely cite the result for

the cross section,

$$\frac{d\sigma}{d^2\mathbf{k}_{a\mathrm{T}}d^2\mathbf{k}_{b\mathrm{T}}dy_a dy_b} = x_a g(x_a,\mu^2)\, x_b g(x_b,\mu^2)\, \frac{d\hat{\Sigma}}{d^2\mathbf{k}_{a\mathrm{T}}d^2\mathbf{k}_{b\mathrm{T}}dy_a dy_b} \qquad (1)$$

where

$$\frac{d\hat{\Sigma}}{d^2\mathbf{k}_{a\mathrm{T}}d^2\mathbf{k}_{b\mathrm{T}}dy_a dy_b} = \frac{4N_{\mathrm{c}}^2\alpha_s^2}{N_{\mathrm{c}}^2-1}\,\frac{1}{k_{a\mathrm{T}}^2}\,2f(\mathbf{q}_{\mathrm{T}},\mathbf{k}_{\mathrm{T}},y_a-y_b)\,\frac{1}{k_{b\mathrm{T}}^2}. \qquad (2)$$

In the first approximation, only gluons can be considered, with densities $g(x,\mu^2)$. The factorization scale is denoted by μ^2. Fractional momenta of the incoming gluons are x_a and x_b, which in the multi-Regge kinematics become

$$x_a \approx \frac{k_{a\mathrm{T}}}{\sqrt{s}}\,\mathrm{e}^{\,y_a}, \qquad\qquad x_b \approx \frac{k_{b\mathrm{T}}}{\sqrt{s}}\,\mathrm{e}^{\,-y_b}. \qquad (3)$$

With the tagging jets the calculation is well defined, since large transverse momenta are required for the tagging jets so that the coupling of the ladder to the jets becomes perturbative. In this case one can still rely on collinear factorization and use the integrated parton densities $xg(x,\mu^2)$. Another important point in this calculation is that when all the radiative and virtual corrections are neglected, one is left with the inhomogeneous term of the BFKL equation only. At this limit the ladder shrinks into $2f(\mathbf{q}_{\mathrm{T}},\mathbf{k}_{\mathrm{T}},y)\to\delta^{(2)}(\mathbf{q}_{\mathrm{T}}-\mathbf{k}_{\mathrm{T}})$, and the Born limit for the two jets separated by a large rapidity interval is recovered [29].

Within the framework of tagging jets, also more exclusive minijet processes have been studied by drawing a minijet out of the ladder [22]. It is straightforward to show that after pulling out a minijet, the gluon emissions before and after the chosen minijet can be summed, resulting as a pomeron ladder on each side of the pulled minijet, as illustrated in Fig. 2. The cross section at the parton level becomes [22]

$$\frac{d\hat{\Sigma}}{d^2\mathbf{k}_{a\mathrm{T}}d^2\mathbf{k}_{b\mathrm{T}}d^2\mathbf{k}_{c\mathrm{T}}dy_a dy_b dy_c} = \frac{4N_{\mathrm{c}}^2\alpha_s^2}{N_{\mathrm{c}}^2-1}\,\frac{\alpha_s N_{\mathrm{c}}}{\pi^2}\,\frac{1}{k_{c\mathrm{T}}^2}\int d^2\mathbf{q}_{1\mathrm{T}}d^2\mathbf{q}_{2\mathrm{T}}\cdot$$

$$\cdot\,\delta^{(2)}(\mathbf{k}_{c\mathrm{T}}-\mathbf{q}_{1\mathrm{T}}+\mathbf{q}_{2\mathrm{T}})\,\frac{2f(\mathbf{k}_{a\mathrm{T}},\mathbf{q}_{1\mathrm{T}},y_a-y_c)}{k_{a\mathrm{T}}^2}\,\frac{2f(\mathbf{q}_{2\mathrm{T}},\mathbf{k}_{b\mathrm{T}},y_c-y_b)}{k_{b\mathrm{T}}^2}, \qquad (4)$$

where the minijet drawn from the middle of the pomeron ladder is labelled as c. The factor $\alpha_s N_{\mathrm{c}}/(\pi^2 k_{c\mathrm{T}}^2)$ is a combination of the phase-space factor and the two Lipatov vertices associated with the step c. The factors 2 are related to the normalization of the ladder f as in Eq. (2). Again, if the radiative and

virtual corrections in the ladder are neglected, one recovers the Born limit for production of three jets well separated in rapidity [29].

What we do in the following is that we simply relax the requirement of having tagging jets, since we want to study the leading BFKL minijet production mechanism, which is $\sim \alpha_s$. This means, unfortunately, that coupling of the pomeron ladder to the hadron becomes essentially soft in $q_{\rm T}$ and $k_{\rm T}$, *i.e.* non-perturbative. This in turn results in the fact that while the other leg of the ladder is coupled to one constituent of the incoming hadron, in the squared graph the other leg may be coupled to another constituent, as shown in Fig. 3. This is nicely illustrated in a classic paper [16] where photon-photon scattering via heavy quarks was studied. Also, now that we do not require any tagging jets we have to give up collinear factorization, and, for the forward scattering amplitude, we do not have a perturbative Born limit to compare with, either. Therefore, the best we can do is to adopt the procedure for deep inelastic scattering in [20], where an addition of each rung into the pomeron ladder between the two hadrons or nuclei is expected to be described by the *homogeneous* BFKL equation. Justification for using a homogeneous evolution equation is that the x-dependence of the hadron form factor describing coupling of the gluon ladder to the hadron is negligible with respect to the x-dependence generated by the BFKL evolution [16].

The homogeneous BFKL equation for the unintegrated gluon densities $f(x, q_{\rm T}^2)$ given in [20], which we will utilize in our problem, can be derived from the homogeneous BFKL equation for $f(\mathbf{q}_{\rm T}, \mathbf{k}_{\rm T}, y)$ in [15, 21] by first integrating over the last momentum exchange $\mathbf{k}_{\rm T}$ in the pomeron ladder, then scaling with $q_{\rm T}^2$ and integrating over the azimuthal angle in the kernel, setting $y = \log(1/x)$ and finally scaling with x. The BFKL equation then becomes [20]

$$-x\frac{\partial f(x,q_{\rm T}^2)}{\partial x} = \frac{\alpha_s N_{\rm c}}{\pi} q_{\rm T}^2 \int_0^\infty \frac{dq_{1{\rm T}}^2}{q_{1{\rm T}}^2}\left[\frac{f(x,q_{1{\rm T}}^2) - f(x,q_{\rm T}^2)}{|q_{\rm T}^2 - q_{1{\rm T}}^2|} + \frac{f(x,q_{\rm T}^2)}{\sqrt{q_{\rm T}^4 + 4q_{1{\rm T}}^4}}\right]. \quad (5)$$

The above equation is scale-invariant, so that additional information for fixing the normalization of the $f(x, q_{\rm T}^2)$ is needed. The integrated gluon densities of a proton, determined through the global analysis of parton distributions [20], will provide us with this input:

$$xg(x,Q^2) = \int^{Q^2} \frac{dq_{\rm T}^2}{q_{\rm T}^2} f(x, q_{\rm T}^2). \quad (6)$$

It should be noted that the non-perturbative nature of the pomeron-hadron coupling is now hidden into the initial $q_{\rm T}^2$-distribution $f(x_0, q_{\rm T}^2)$, which must

be supplied at fixed $x_0 \leq 0.01$. Equation (5) can then be solved numerically to obtain $f(x, q_{\rm T}^2)$. In our discussion we will return to the treatment of the infrared problems of Eq. (5) but here will rely on the analysis of [20].

Now we are ready to write down the formula for inclusive minijet production from the BFKL pomeron ladder between the two colliding hadrons (nuclei) as illustrated in Fig. 3. Based on Eq. (4), we get the factor $\alpha_s N_{\rm c}/(\pi^2 p_{\rm T}^2)$ when pulling out a minijet by fixing the momentum of one rung of the pomeron ladder. When doing this we form a new ladder on each side of the minijet. The coupling of these ladders to the hadrons or nuclei is contained in the initial condition for the unintegrated gluon distribution $f(x, q^2)$, as explained above. Then, the cross section for inclusive minijet production is bound to have the same structure as in Eq. (4), and one obtains [18, 19]

$$\frac{d\sigma^{\rm jet}}{d^2\mathbf{p}_{\rm T} dy} = K_N \frac{\alpha_s N_{\rm c}}{\pi^2} \frac{1}{p_{\rm T}^2} \int d^2\mathbf{q}_{1\rm T} d^2\mathbf{q}_{2\rm T}\, \delta^{(2)}(\mathbf{p}_{\rm T} - \mathbf{q}_{1\rm T} + \mathbf{q}_{2\rm T}) \frac{f(x_1, q_1^2)}{q_{1\rm T}^2} \frac{f(x_2, q_2^2)}{q_{2\rm T}^2} \tag{7}$$

where $p_{\rm T}$ and y are the transverse momentum and the rapidity (in the hadron CMS) of the minijet. From momentum conservation and multi-Regge kinematics the momentum fractions become

$$x_1 \approx \frac{p_{\rm T}}{\sqrt{s}} \mathrm{e}^{\,y}, \qquad x_2 \approx \frac{p_{\rm T}}{\sqrt{s}} \mathrm{e}^{-y}. \tag{8}$$

Due to the fact that in this case we do not have an "external" hard probe like the virtual photon with an associated quark box as in DIS, nor an on-shell Born cross section to relax into, we cannot determine the overall dimensionless normalization constant K_N exactly. However, we are able to fix the *slope* of the minijet $p_{\rm T}$-distribution. Then, based on this slope we will discuss the upper bound for K_N and actually argue that $K_N \lesssim 1$. It is possible that an analysis of two-jet emission will clarify this issue. This demands in fact considering a $k_{\rm T}$-factorized form of the two-jet production cross section [30]. By comparing this rate with the one evaluated directly from the BFKL ladder one would hope to get an absolute normalization to the off-shell gluon flux.

Instead of numerically solving the homogeneous BFKL equation (5), we will use a simple parametrization for the solution, motivated by the form of the solution in the limit of asymptotically small x [16, 20]:

$$f(x, q_{\rm T}^2) = \frac{C}{x^\lambda} \left(\frac{q_{\rm T}^2}{q_0^2}\right)^{\frac{1}{2}} \frac{\bar{\varphi}_0}{\sqrt{2\pi\lambda'' \ln(1/x)}} \exp\Big[-\frac{\ln^2(q_{\rm T}^2/\bar{q}^2)}{r 2\lambda'' \ln(1/x)}\Big]. \tag{9}$$

In this expression $\lambda = 4\bar{\alpha}_s \ln 2$, $\lambda'' = 28\bar{\alpha}_s\zeta(3)$, $\bar{\alpha}_s = 3\alpha_s/\pi$, $\zeta(3) = 1.202$ is the Riemann zeta function and $\bar{\varphi}_0$, q_0 and $\bar{q}$ are parameters characterizing the initial distribution in [20]. We reproduce the width of the solution with

an additional parameter r. For definiteness we shall take $\alpha_s = 0.2$, resulting in the same slope ($\sim x^{-0.5}$) as in the MRSD-' set of parton distributions [31]. By choosing $\bar{q} = q_0 = 1$, $C\bar{\varphi} = 1.19$ and $r = 0.15$, the proposed parametrization (9) describes with a satisfactory accuracy the gluon distribution, which is obtained as the numerical solution of the BFKL equation in the global analysis [20][3]. For comparison with Ref. [20], we show the unintegrated gluon distributions of Eq. (9) in Fig. 4 as functions of $q_{\rm T}^2$ at different values of x.

Proceeding then to the computation of the minijet cross sections, we integrate over the azimuthal angle between $\mathbf{p}_{\rm T}$ and $\mathbf{q}_1$ in Eq. (7) and fix $K_N = 1$ and $y = 0$. Results for the minijet cross sections $d\sigma^{\rm jet}/(dp_{\rm T}dy)$ at the LHC heavy-ion energy $\sqrt{s} = 5.5$ TeV and at the UA1 energy $\sqrt{s} = 900$ GeV are shown in Figs. 5a and b. These are the main results of this paper. The corresponding cross sections from the more conventional, collinearly factorized leading twist lowest order (CFLTLO) $2 \to 2$ mechanism (see [9]) with the MRSD-' parton distributions, are also shown for comparison. In the MRSD-' parton distribution functions we have made a scale choice $Q = p_{\rm T}$, so we can only proceed down to $p_{\rm T} = \sqrt{5}$ GeV, the lowest scale for this set. With the BFKL mechanism, we extend our computation down to 1 GeV. Note also that no K-factor to simulate the next-to-leading order (NLO) terms is used for the CFLTLO computation.

In the BFKL approach only gluons are considered, and we have fixed $\alpha_s = 0.2$ in Eq. (7). In order to compare the two production mechanisms at the same level of approximation, we also plot the corresponding curves for the collinearly factorized results. However, since in the analysis of $f(x, q_{\rm T}^2)$ in [20], the strong coupling constant was set to run — phenomenologically, because NLO corrections to the BFKL ladder are not yet known — we show also the BFKL result with $\alpha_s(p_{\rm T})$.

Let us then come to the question of the normalization constant K_N. We expect the BFKL mechanism to be valid and potentially important only at $x < 0.01$, where the rapid rise of the structure function $F_2(x, Q^2)$ is observed [7, 8]. Based on Eq. (8), the region of validity would then be $p_{\rm T} < 9$ GeV for $\sqrt{s} = 900$ GeV at $y = 0$ in Fig. 5b. On the other hand, the experimentally measured jet cross sections at $p_{\rm T} > 5.5$ GeV [32] can be explained through the collinear factorization mechanism for jet production rather than through the BFKL mechanism considered here. When the next-to-leading order corrections to CFLTLO jet cross section are included, the measured jet cross sections are well reproduced [33, 34]. Let us also note that with a scale choice $Q = p_{\rm T}$ the NLO calculation can be reproduced by multiplying the Born level cross section by a factor between 2 and 1.5, depending on $\sqrt{s}$

[3]We are grateful to D.M. Ostrovsky for a numerical check of this statement.

and on the size of the jet [34]. This tells us that there is no room for an *additional* jet production mechanism of the same order of magnitude. Given this, and comparing the two mechanisms at the same level of approximation, the conclusion from Fig. 5b is that the BFKL mechanism in Eq. (7) can indeed at most have $K_N \sim 1$. In fact, this provides an upper bound for the non-leading BFKL corrections as well.

Up to this point, everything we have considered applies to pp collisions. The first estimate, without nuclear modifications to the parton densities, of the average number distributions of produced semihard gluons in central AA collisions can be obtained simply by multiplying the results in Fig. 5 by the nuclear overlap function, $T_{AA}(\mathbf{b} = \mathbf{0}) \approx A^2/(\pi R_A^2)$ [3]. For central Pb-Pb collisions, $T_{\rm PbPb}(\mathbf{0}) = 32/\text{mb}$.

As the last step, we estimate the transverse energy production due to the BFKL minijets in nuclear collisions. From the point of view of quark-gluon-plasma formation, and of its further evolution, we are mostly interested in the transverse energy deposit into the central rapidity region $y \sim 0$. An estimate for the rapidity distribution of the average transverse energy in an AA collision at an impact parameter $\mathbf{b} = \mathbf{0}$ is obtained as

$$\left.\frac{d\bar{E}_{\rm T}^{AA}}{dy}\right|_{y=0} = T_{AA}(\mathbf{b}) \int_{p_0} dp_{\rm T} p_{\rm T} \left.\frac{d\sigma^{\rm jet}}{dp_{\rm T} dy}\right|_{y=0}. \tag{10}$$

Since the minijet cross sections computed for Fig. 5 are approximately constant at rapidities $|y| < 0.5$, Eq. (10) also gives a good estimate for the transverse energy deposit into the central unit of rapidity. By using the BFKL cross sections in Fig. 5 with $p_0 = 1$ GeV we obtain the results shown in Table 1 for the LHC heavy-ion energy $\sqrt{s} = 5.5\,A$TeV. Again, comparison with the CFLTLO results with $p_0 = \sqrt{5}$ GeV is made in this table. We remind the reader that the numbers quoted for the BFKL minijets are with $K_N = 1$ and we do not make any attempt to include nuclear modifications [11, 12] in any of the gluon distributions considered.

Concerning our results, we would like to point out the following observations:

1. Although the BFKL mechanism we have considered here is leading in powers of α_s – BFKL $\sim \alpha_s$ and CFLTLO $\sim \alpha_s^2$ – and although the transverse momenta in the BFKL ladder have enlarged phase-space in the sense that they are not ordered as in the DGLAP-ladder, it is not enough to overcome the CFLTLO contribution at $p_{\rm T} \geq p_0 \sim 2$ GeV.

2. The slopes of the BFKL and CFLTLO computations in Fig. 5 are quite similar at large $p_{\rm T}$. This demonstrates that at fixed $\sqrt{s}$ the relevant physical scale is the transverse momentum $p_{\rm T}$. Since the gluon distributions have the slope $\sim x^{-0.5}$ and since $x \sim p_{\rm T}/\sqrt{s}$, the jet cross sections scale as

$d\bar{E}_{\rm T}^{\rm PbPb}/dy$ $y=0$, $\mathbf{b}=0$	BFKL $K_N=1$, $p_0=1$ GeV	CFLTLO glue only, $p_0=\sqrt{5}$ GeV
$\alpha_s=0.2$	3060 GeV	3060 GeV
$\alpha_s=\alpha_s(p_{\rm T})$	4940 GeV	4870 GeV

Table 1: The average transverse energy at $y=0$ carried by minijets with $p_{\rm T}\geq p_0$ in central Pb-Pb collisions at $\sqrt{s}=5.5$ ATeV.

$d\sigma^{\rm jet}/dp_{\rm T}\sim(x_1x_2)^{-0.5}/p_{\rm T}^3\sim\sqrt{s}/p_{\rm T}^4$ for both mechanisms.

Let us next discuss the potential caveats and uncertainties. As discussed above, due to the non-perturbative coupling of the pomeron to the hadrons or nuclei, and lacking the corresponding partonic Born process as a special limiting case, we were able to fix the slope of the minijet production only, not the absolute magnitude. Based then on the measured jet cross sections [32] and the collinearly factorized calculations, we argued that the production of minijets through the BFKL mechanism can at most be compatible with minijet production in the collinear factorization approach [9].

However, both approaches have problems when $p_{\rm T}\to 0$, which we did not discuss above. At this limit the CFLTLO cross sections grow rapidly, and, especially with the HERA parton distributions, it is not plausible to go much below $p_{\rm T}=p_0\sim 2$ GeV since this leads to an overprediction of the measured charged hadron distributions [35].

On the other hand, also the BFKL approach has serious infrared problems. As seen in Eq. (5), a contribution to the BFKL evolution comes from the soft region $q_{\rm T}<q_{\rm T}^0\sim 1$ GeV, the importance of which is enhanced if a running coupling is used. The infrared region was treated in [20] by introducing an x-independent form factor at $q_{\rm T}<q_{\rm T}^0=1$ GeV together with $\alpha_s(q_{\rm T}^2)$. For a more detailed discussion, we refer to [20] and references therein. We believe that in spite of this phenomenological input in the soft sector, the correct order of magnitude of the BFKL results can be obtained since, first, the high-$q_{\rm T}^2$ region can be computed perturbatively from the BFKL equation and, second, the normalization of the unintegrated gluon distributions to the integrated ones can be made. We would also expect that if the BFKL mechanism is indeed the reason for the rapid rise of the HERA parton densities at

small x, it could dominate the minijet production in the region of $p_{\rm T} < p_0$, where the CFLTLO calculation does not apply.

The subleading contributions are not yet known for the BFKL approach, although the work is currently in progress [36]. For the $2 \to 2$ cross sections of massless partons, the NLO terms have already been known for a while [37], and they have been applied to the case of jet production [33]. However, one should keep in mind that minijet production is conceptually different from the jet production since minijets are not observed as individual jets. For minijets the NLO analysis can be made for infrared-safe quantities, such as the transverse energy deposit in $|y| \leq 0.5$. This task has not been completed yet. Especially, it remains to be seen what the scale dependence of the transverse energy deposit turns out to be.

The last potential caveat, well hidden in our BFKL approach[4], is related to the inclusive and more exclusive processes. In [21], the calculation is well defined, since the minijet production considered is fully inclusive. One finds a complete cancellation of infrared singularities between the virtual and real emissions in the pomeron ladder, leading to the explicit form of the kernel in Eq. (5). When the coherence of the ladder is broken by extracting a minijet, a potential problem with the exclusiveness and the cancellation of the singularities arises (see [38]). At the moment we do not know precisely how to address this problem. However, since we are computing semi-inclusive quantities, in particular the transverse energy flow with less infrared-sensitivity, we believe that our estimates of the magnitude of minijet production with $p_T \geq 1$ GeV and of the associated $\bar{E}_T^{AA}$ in $|y| \leq 0.5$ are reliable.

Finally, we would like to discuss the connection to other studies. Recently, there has been a lot of activity in developing an approach to semihard parton production in ultrarelativistic heavy-ion collisions, based on an idea of colour charge distributions of the nuclear valence quarks moving along the light cone and creating clouds of virtual gluons around them [27]. In this approach, production of semihard quanta will result from a collision of two such incoming clouds. The leading mechanism of minijet production would then obviously be through $2 \to 1$ processes, *i.e.* of order α_s, not α_s^2 as in the collinearly factorized mechanism. Conceptually, this may be similar to the BFKL mechanism we have considered here, although, to our knowledge, an exact relation is not known at the moment.

To summarize, we have computed minijet production from a BFKL pomeron ladder and estimated the transverse energy production in the midrapidity in a central Pb-Pb collision at $\sqrt{s} = 5.5$ ATeV. We have used unintegrated gluon densities similar to those of Ref. [20], so as to show that

[4]We thank Yu. Dokshitzer for pointing this out.

the BFKL contribution is at most of the same order of magnitude as the collinearly factorized one in the considered region. However, with the BFKL mechanism one could be able to bridge the way into the region $p_{\rm T} < p_0$ in a manner at least partly controlled by perturbative QCD.

Acknowledgements: We are grateful to Yu. Dokshitzer, K. Kajantie, E. Laenen, L. McLerran and H. Satz for useful discussions. We would also like to thank Nordita for hospitality during part of this work and the Finnish Academy (K.J.E.) for financial support. The work of A.V.L. was partially supported by the Russian Fund for Basic Research, Grant 93-02-3815.

References

[1] T. K. Gaisser and F. Halzen, Phys. Rev. Lett. **54** (1985) 1754; G. Pancheri and Y. N. Srivastava, Phys. Lett. **B182** (1986) 199; L. Durand and H. Pi, Phys. Rev. Lett. **58** (1987) 303; R. C. Hwa, Phys. Rev. **D37** (1988) 1830.

[2] X.-N. Wang, Phys. Rev. **D43** (1991) 104.

[3] K. Kajantie, P. V. Landshoff and J. Lindfors, Phys. Rev. Lett. **59** (1987) 2517; K.J. Eskola, K. Kajantie and J. Lindfors, Nucl. Phys. **B323** (1989) 37.

[4] X.-N. Wang and M. Gyulassy, Phys. Rev. **D44** (1991) 3501; *ibid.* **D45**, 844 (1992) 844; Phys. Rev. Lett. **68** (1992) 1480; Comput. Phys. Commun. **83** (1994) 307.

[5] K. Geiger and B. Müller, Nucl. Phys. **B369** (1992) 600; K. Geiger, Phys. Rev. **D47** (1993) 133.

[6] J.P. Blaizot and A.H. Mueller, Nucl. Phys. **B289** (1987) 847.

[7] H1 Collaboration, I. Abt *et al.*, Nucl. Phys. **B407** (1993) 515; H1 Collaboration,T. Ahmed *et al.*, Nucl. Phys. **B439** (1995) 471; ZEUS Collaboration, M. Derrick *et al.*, Phys. Lett. **B316** (1993) 412; Z. Phys. **C65** (1995) 379.

[8] H1 Collaboration, S. Aid *et al.*, Preprint DESY 96-039, March 1996.

[9] K.J. Eskola, K. Kajantie and P.V. Ruuskanen, Phys. Lett. **B332** (1994) 191; K.J. Eskola, in Proc. of *Quark Matter '95*, eds. A.M. Poskanzer *et al.*, Nucl. Phys. **A590** (1995) 383c.

[10] EM Collaboration, M. Arneodo *et al.*, Nucl. Phys. **B333** (1990) 1; NM Collaboration, P. Amaudruz *et al.*, Z. Phys. **C51** (1991) 387; E665 Collaboration, M.R. Adams *et al.*, Phys. Rev. Lett. **68** (1992) 3266.

[11] K.J. Eskola, Nucl. Phys. **B400** (1993) 240.

[12] K.J. Eskola, J. Qiu and X.-N. Wang, Phys. Rev. Lett. **72** (1994) 36.

[13] Yu. Dokshitzer, Sov. Phys. JETP **46** (1977) 1649; V. N. Gribov and L. N. Lipatov, Sov. Nucl. Phys. **15** (1972) 438, 675; G. Altarelli, G. Parisi, Nucl. Phys. **B126** (1977) 298.

[14] R. D. Ball and S. Forte, Phys. Lett. **B351** (1995) 313; Phys. Lett. **B359** (1995) 362; Phys. Lett. **B336** (1994) 77.

[15] E. A. Kuraev, L. N. Lipatov and V. S. Fadin, Sov. Phys. JETP **45** (1977) 199.

[16] Ya. Ya. Balitskij and L. N. Lipatov, Sov. J. Nucl. Phys. **28** (1978) 822.

[17] J. Kwieciński, A. D. Martin, W. J. Stirling and R. G. Roberts, Phys. Rev. **D42** (1990) 3645.

[18] L. V. Gribov, E. M. Levin and M. G. Ryskin, Phys Lett. **B100** (1981) 173; Phys Lett. **B121** (1983) 65; Phys. Rep. **100** (1983) 1; E. M. Levin and M. G. Ryskin, Phys. Rep. **189** (1990) 267.

[19] E. Laenen and E. Levin, Annu. Rev. Nucl. Part. Sci. **44** (1994) 199.

[20] A. J. Askew, J. Kwieciński, A. D. Martin and P. J. Sutton, Phys. Rev. **D49** (1994) 4402.

[21] A. H. Mueller and H. Navelet, Nucl. Phys **B282** (1987) 727.

[22] V. Del Duca, M. E. Peskin and W.-K. Tang, Phys. Lett. **B306** (1993) 151.

[23] V. T. Kim and G. B. Pivovarov, Phys. Rev. **D53** (1996) R6.

[24] R. Ragazzon and D. Treleani, Phys. Rev. **D53** (1996) 55.

[25] K. Golec-Biernat, J. Kwieciński, A. D. Martin and P. J. Sutton, Phys. Lett. **B335** (1994) 220; J. Kwieciński, A. D. Martin, P. J. Sutton and K. Golec-Biernat, Phys. Rev. **D50** (1994) 217.

[26] E. Laenen and E. Levin, J. Phys. **G19** (1993) 1582.

[27] R. Venugopalan, in Proc. of *Quark Matter '95*, eds. A.M. Poskanzer *et al.*, Nucl. Phys. **A590** (1995), R. Venugopalan, Preprint DOE/ER/ 40561-251-INT96-00-120, March 1996; A. Kovner, L. Mc Lerran and H. Weigert, Phys. Rev. **D52** (1995) 3809, 6231.

[28] A. Donnachie and P. V. Landshoff, Phys. Lett. **B332** (1994) 433.

[29] V. Del Duca, "An introduction to the perturbative QCD pomeron and to jet physics at large rapidities", DESY 95-023, February 1995.

[30] S. Catani, M. Ciafaloni and F. Hautmann, Phys. Lett. **B242** (1990) 97; Nucl. Phys. **B366** (1991) 135; J. C. Collins and R. K. Ellis, Nucl. Phys. **B360** (1991) 3.

[31] A. D. Martin, W. J. Stirling and R. G. Roberts, Phys. Lett. **B306** (1993) 145.

[32] UA1 Collaboration, C. Albajar *et al.*, Nucl. Phys. **B309** (1988) 405.

[33] S. D. Ellis, Z. Kunszt and D. E. Soper, Phys. Rev. Lett. **62** (1989) 726; Phys. Rev. **D40** (1989) 2188; Phys. Rev. Lett. **69** (1992) 1496; Z. Kunszt and D. E. Soper, Phys. Rev. **D46** (1992) 192.

[34] K.J. Eskola and X.-N. Wang, "High $p_{\rm T}$ jet production in pp collisions", in *Hard processes in hadronic interactions,* eds. H. Satz and X.-N. Wang, Int. J. Mod. Phys. **A10** (1995) 2881.

[35] UA1 Collaboration, C. Albajar *et al.*, Nucl. Phys. **B335** (1990) 261.

[36] V. S. Fadin, L. N. Lipatov, Preprint DESY 96-020, Feb 1996; V. Del Duca, Preprint DESY 95-249, January 1996; Preprint EDINBURGH 96/3, April 1996.

[37] R. K. Ellis and J. C. Sexton, Nucl. Phys. **B269** (1986) 445.

[38] G. Marchesini, Nucl. Phys. **B445** (1995) 49.

Figure Captions

Fig. 1. Fully inclusive minijet production with tagging jets a and b [21]. The BFKL pomeron ladder is denoted by $f(\mathbf{q}_{\rm T}, \mathbf{k}_{\rm T}, y_a - y_b)$, and only the cut ladder is shown. The thick lines represent the exponentiated gluon propagators and the black blobs stand for the effective non-local Lipatov vertices.

Fig. 2. Production of minijet c from the cut BFKL pomeron ladder of Fig. 1 [22]. A new ladder arises on each side of the minijet.

Fig. 3. Production of minijets from the cut BFKL pomeron ladder without tagging jets. The ovals with one thick line and three thin ones attached represent the incoming protons, and $f(x_{1(2)}, q^2_{1(2)\rm T})$ describe the BFKL pomeron ladders obeying Eq. (5). For details, see the text. The cross section for minijet production through this mechanism is given in Eq. (7).

Fig. 4. The unintegrated gluon distributions $f(x, q^2_{\rm T})$ divided by $\sqrt{q^2_{\rm T}}$ as given by the parametrization in Eq. (9) as a function of $q^2_{\rm T}$. The curves correspond to three different, fixed values of x.

Fig. 5. a. Cross sections $d\sigma^{\rm jet}/(dp_{\rm T}dy)$ at $y = 0$ as functions of $p_{\rm T}$ for $\sqrt{s} = 5.5$ TeV as predicted by Eq. (7). For the BFKL mechanism, two different curves are shown: the solid line corresponds to having fixed $\alpha_s = 0.2$ in Eq. (7), the dashed line corresponds to $\alpha_s = \alpha_s(p_{\rm T})$. For the collinearly factorized leading twist lowest order (CFLTLO) computation [9], we show three different curves: the dash-dotted line is the full computation with all parton flavours and $\alpha_s(p_{\rm T})$, the dashed line is the line with gluons only, and the solid line is obtained with gluons only and $\alpha_s = 0.2$. To see the deviations from scaling limit (see the text), the log-log plot is used.

b. The same as in Fig. 5a, but for $\sqrt{s} = 900$ GeV.

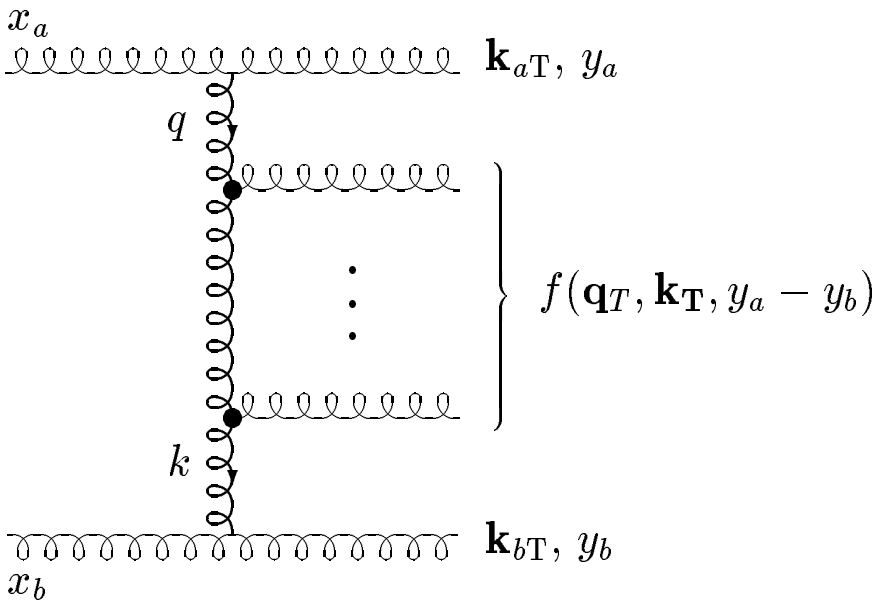
x_a
$\mathbf{k}_{a\mathrm{T}},\ y_a$
q
$f(\mathbf{q}_T, \mathbf{k_T}, y_a - y_b)$
k
$\mathbf{k}_{b\mathrm{T}},\ y_b$
x_b

Fig. 1

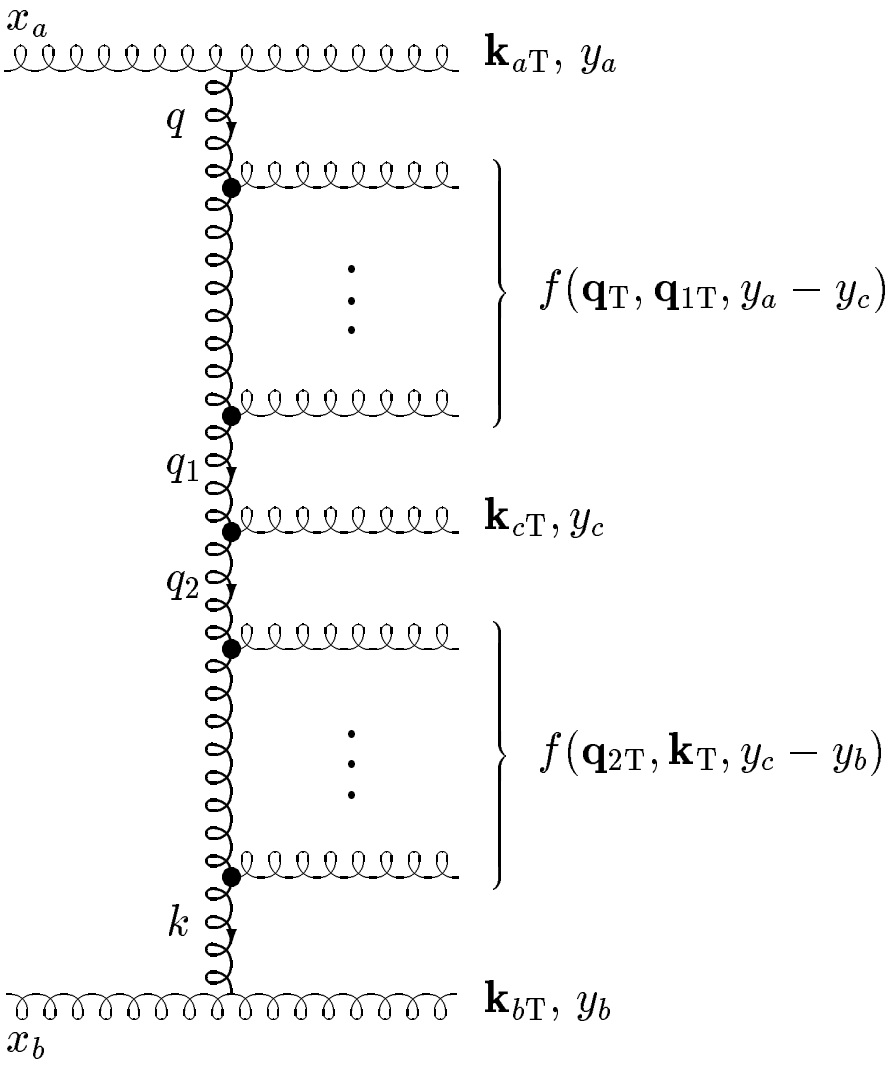
x_a
$\mathbf{k}_{a\mathrm{T}},\ y_a$
q
$f(\mathbf{q}_{\mathrm{T}}, \mathbf{q}_{1\mathrm{T}}, y_a - y_c)$
q_1
$\mathbf{k}_{c\mathrm{T}}, y_c$
q_2
$f(\mathbf{q}_{2\mathrm{T}}, \mathbf{k}_{\mathrm{T}}, y_c - y_b)$
k
$\mathbf{k}_{b\mathrm{T}},\ y_b$
x_b

Fig. 2

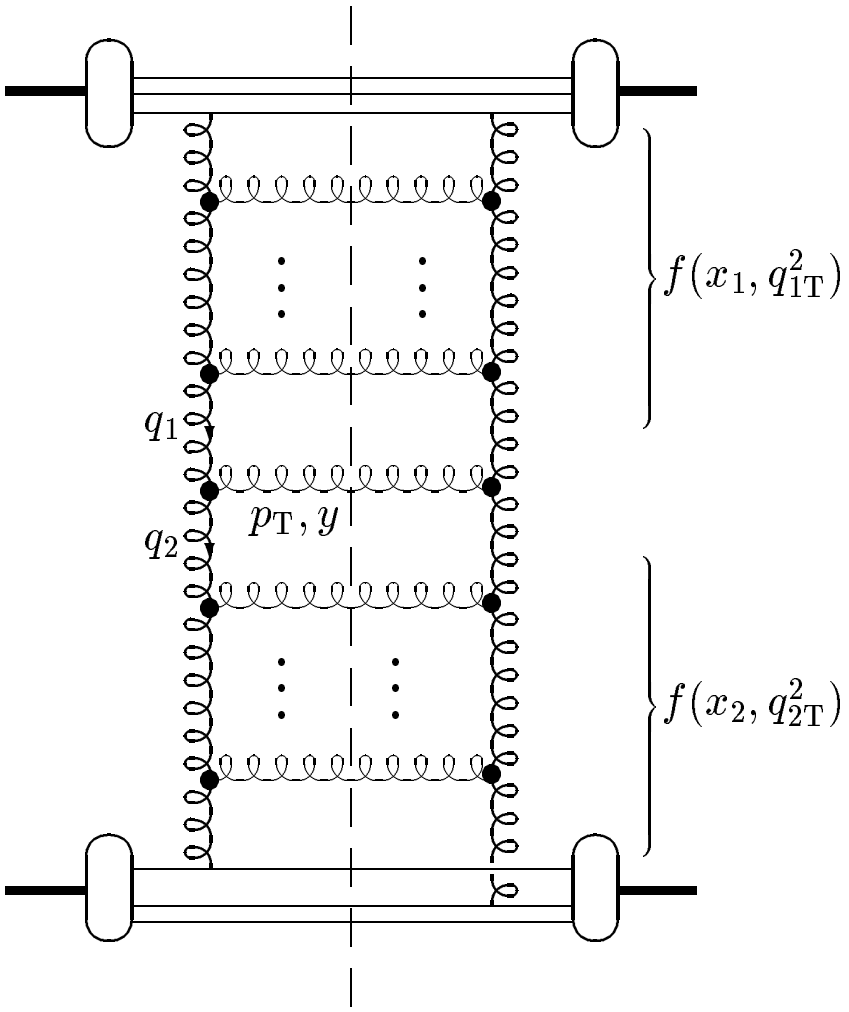

Fig. 3

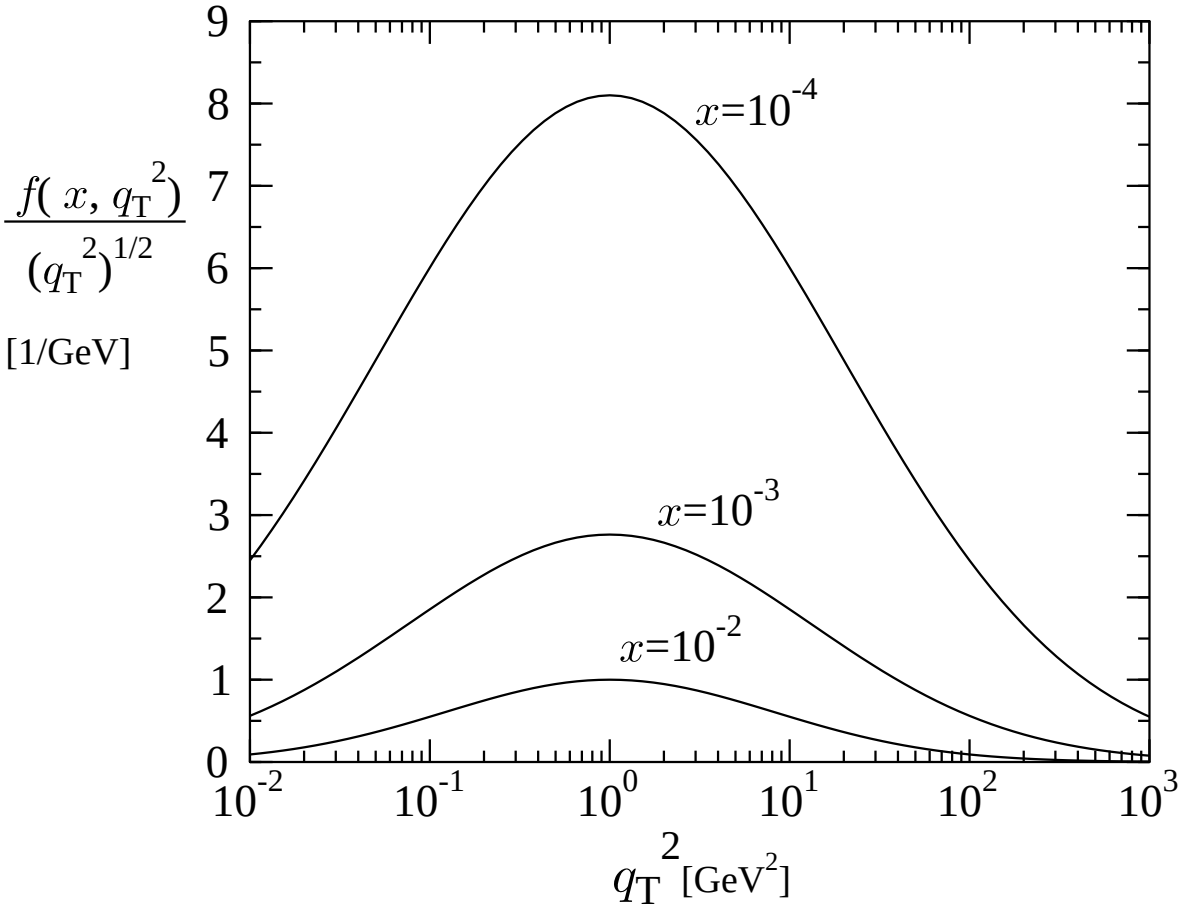
$\frac{f(x, q_T^2)}{(q_T^2)^{1/2}}$
[1/GeV]
9
8
7
6
5
4
3
2
1
0
$x=10^{-4}$
$x=10^{-3}$
$x=10^{-2}$
10^{-2}
10^{-1}
10^{0}
10^{1}
10^{2}
10^{3}
q_T^2 [GeV^2]

Fig. 4

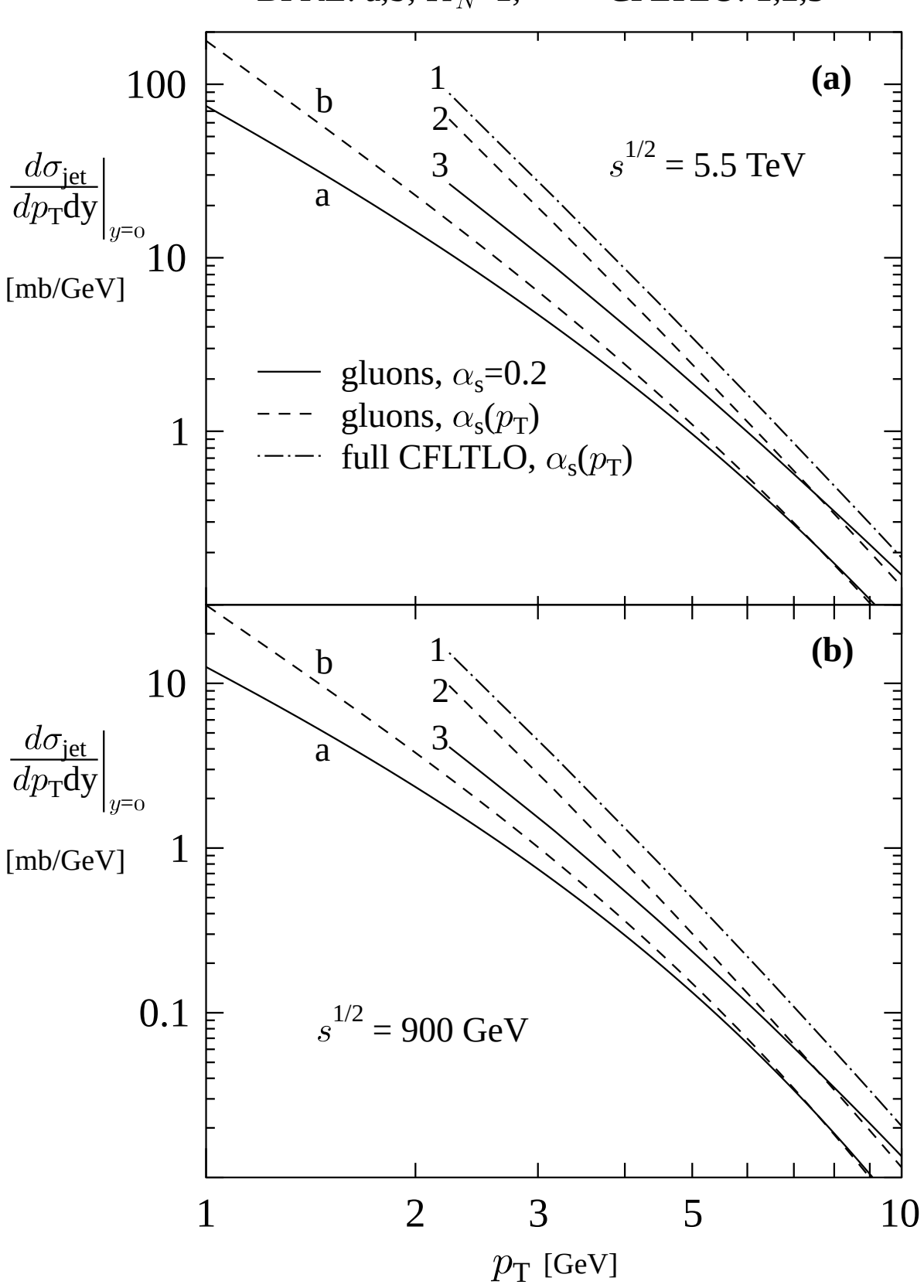
BFKL: a,b; K_N=1,
CFLTLO: 1,2,3
(a)
(b)
$s^{1/2}$ = 5.5 TeV
$s^{1/2}$ = 900 GeV
gluons, α_s=0.2
gluons, $\alpha_s(p_T)$
full CFLTLO, $\alpha_s(p_T)$
$\frac{d\sigma_{jet}}{dp_T dy}\Big|_{y=0}$
[mb/GeV]
p_T [GeV]
100
10
1
0.1
1
2
3
5
10
a
b
1
2
3

Fig. 5